Radiating Barotropic Instability

L. D. TALLEY

School of Oceanography, Oregon State University, Corvallis, 97331

(Manuscript received 14 January 1983, in final form 22 February 1983)

ABSTRACT

The linear stability of zonal, parallel shear flow on a beta-plane is discussed. While the localized shear region supports unstable waves, the far-field can support Rossby waves because of the ambient potential-vorticity gradient. An infinite zonal flow with a continuous cross-stream velocity gradient is approximated with segments of uniform flow, joined together by segments of uniform potential vorticity. This simplification allows an exact dispersion relation to be found. There are two classes of linearly unstable solutions. One type is trapped to the source of energy and has large growth rates. The second type is weaker instabilities which excite Rossby waves in the far-field: the influence of these weaker instabilities extends far beyond that of the most unstable waves.

1. Introduction

The large-scale eddy energy distribution in mid-latitude oceans is highly inhomogeneous. It is quite clear from the spatial distribution of energy (Dantzler, 1977) that intense ocean currents are the source of a large part of the eddy energy and thus its spatial inhomogeneity. However, the scale of meridional decay of energy away from the zonal portions of these currents is too slow to be accounted for by the most unstable waves of the currents, since their decay scales are not much larger than the internal Rossby deformation radius. An explanation of the slow decay is sought here and in an accompanying paper (Talley, 1983) in the form of "radiating," quasi-geostrophic instabilities of zonal currents. These instabilities have large meridional decay scales but somewhat lower growth rates than the most unstable waves. It is hypothesized that the fully developed eddy field in a broad neighborhood of the currents is composed of the most unstable, most trapped waves directly in the current with a gradual shift to less unstable, radiating instabilities in the far-field. Because the stability problems considered in these papers are linear, it is not known whether this hypothesis is true. However, the theory is qualitatively consistent with data in the western North Atlantic (Talley).

This paper considers the stability of zonal, barotropic shear-flows and jets. While the most general currents in the ocean and atmosphere have both horizontal and vertical shear, the existence of strong horizontal shear in the ocean and atmosphere suggests that in some circumstances barotropic instability may be important. It is also useful to understand the barotropic and baroclinic stability problems separately before combining them, as is done by Talley (1983). Direct comparison of the theoretical results with oceanic observations is also given by Talley.

The stability of parallel shear flow was initially considered in the nineteenth century. Piecing flow profiles from straight lines, Rayleigh (1879, 1880) obtained analytic solutions for a variety of cases, including shear layers and jets, with and without zonal boundaries. He also derived a necessary condition for instability based on the occurrence of an inflection point in the velocity distribution (Rayleigh, 1887). A second necessary condition for instability of parallel shear flow was derived by Fjørtoft (1950).

The stability of parallel shear flows in the presence of a variable Coriolis parameter was first studied by Kuo (1949). The stability of parallel shear flows on the β-plane was also investigated by Howard and Drazin (1964) who found analytic solutions for simple flow profiles and a neutral stability curve for the shear flow, $U(y) = \tanh y$. Most importantly for the present investigation, they predicted an additional long-wave mode for the hyperbolic-tangent flow with non-zero β.

Dickinson and Clare (1973) took up the search for the unstable modes of the hyperbolic tangent profile on the β-plane. They confirmed Howard and Drazin's suspicions, finding an additional long-wave mode when β is non-zero. Moreover, they paid close attention to the horizontal structure of the instabilities and found that the unstable waves identified with the hyperbolic tangent instability at $\beta = 0$ are strongly trapped to the shear zone, while the unstable long waves resemble Rossby waves in the westerly part of the flow. They suggested that these "radiating" instabilities, which have large meridional decay scales, can

be interpreted as Rossby waves over-reflected from the shear zone.

The existence of the radiating solutions found by Dickinson and Clare (1973) requires an ambient potential-vorticity gradient (e.g., β) in the outer-field. It also depends crucially on the overlapping of instability phase speeds and zonal wavenumbers with the Rossby-wave phase speeds and zonal wavenumbers of the far-field. McIntyre and Weissman (1978) discussed this phase speed condition; they also discussed the definition and existence of radiating waves. The definition of radiation is extended here to include instabilities which are similar to Rossby waves in the flow external to the energy source.

Since strict limits can be placed on instability phase speeds (Howard, 1961; Pedlosky, 1964) and since the Rossby-wave dispersion relation gives the phase speeds of Rossby waves in the far-field, it is easy to predict when an unstable flow will *not* radiate. Proving the existence of radiating solutions, of course, requires solving the specific problem. Instability phase speeds must be within the range of the mean flow speed (with a small correction due to β) and Rossby-wave phase speeds must be westward with respect to the mean flow. Thus, a monotonic shear layer or a westward jet may radiate, while an eastward, barotropic jet cannot radiate.

A relevant investigation of how neutral (Rossby) waves in a flow with vertical shear can be forced by a moving boundary was made by Pedlosky (1977). Disturbances forced by the boundary were either strongly trapped or purely radiating (semi-infinite Rossby waves), depending on whether the phase speed condition was satisfied. The present papers extend this theory to its motivating situation, namely whether periodic instabilities of a zonal current can excite the ambient waves of the far-field and carry the instabilities' energy far into the ocean interior.

In the context of Kelvin–Helmholtz instability, Lindzen and Rosenthal (1976) showed that, in addition to the usual instabilities that are trapped to the shear layer, there can be unstable, "radiating", internal gravity waves if the buoyancy frequency in the fluid is non-zero. This is equivalent to the existence of a potential vorticity gradient which can support Rossby waves in the present case.

Flow profiles are simplified using Rayleigh's method (1879, 1880) extended to flow on the β-plane. Necessary conditions are derived and a definition of radiating instabilities is given. Unstable solutions of a monotonically sheared flow and a thin jet are found. When β is non-zero, so that there is a potential vorticity gradient throughout the fluid, the instabilities of a monotonically sheared flow and a westward jet radiate and are basically destabilized Rossby waves. An eastward jet cannot radiate outside the jet because the phase speed condition cannot be satisfied.

2. Formulation of the linear-stability program for homogeneous, parallel shear flow

The basic formulation of the shear flow problem is well-known. Rayleigh (1880) derived the governing vorticity equation for non-rotating, homogeneous flow and solved it for many simple cases. The introduction of uniform rotation has no effect on the homogeneous shear-flow problem. If however, the rotation is non-uniform, as it is in a spherical system or in the β-plane approximation to the spherical system, the stability problem is affected because the vorticity gradient of the basic flow is affected. Variable Coriolis parameter was included by Kuo (1949) and Howard and Drazin (1964).

The fluid whose flow is examined for stability is assumed to be homogeneous and inviscid. It is rotating with angular velocity Ω. The local Coriolis parameter is $f = 2\Omega \sin\theta$, where θ is latitude, whose approximately linear variation is equal to β_0. The flow is assumed to have small Rossby number U/fL and is quasi-geostrophic. The velocities are written in terms of a streamfunction Ψ. The non-dimensionalized potential vorticity equation for such a flow is derived and discussed by Pedlosky (1979). It is

$$\left(\frac{\partial}{\partial t} - \Psi_y \frac{\partial}{\partial x} + \Psi_x \frac{\partial}{\partial y}\right)(\nabla^2\Psi + \beta y) = 0. \qquad (1)$$

A length scale L and velocity scale U_0, which are inherent scales of the flow, have been used to non-dimensionalize the equation. Time is non-dimensionalized by LU_0^{-1}. There is one non-dimensional parameter, $\beta = \beta_0 L^2 U_0^{-1}$. It is further assumed that the velocity and stream function are composed of two well separated parts: a mean, steady flow and infinitesimal perturbations on the flow. The basic flow is assumed to be zonal and to vary only with latitude. Thus

$$\left.\begin{aligned} \Psi &= \psi(y) + \phi(x, y, t) \\ u &= U(y) + u'(x, y, t) = -\frac{\partial \psi}{\partial y} - \frac{\partial \phi}{\partial y} \\ v &= v'(x, y, t) = \phi_x \end{aligned}\right\},$$

where $\phi \ll \psi$. Linearizing the potential vorticity equation (1) to include only terms of order $|\phi|$, we obtain

$$\left(\frac{\partial}{\partial t} + U(y)\frac{\partial}{\partial x}\right)\nabla^2\phi + \phi_x(\beta - U_{yy}) = 0.$$

The domain of the flow is infinite in the x-direction and may be bounded by walls at $y = \pm H$. The boundary condition at $y = \pm H$ is that $v = \phi_x = 0$. If $H \to \infty$, the boundary condition is that the solution be bounded at infinity, or equally that the energy flux be outward at infinity.

Seeking normal mode solutions

$$\phi(x, y, t) = A(y)e^{ik(x-ct)},$$

where k is real and $A(y)$ and c are complex, the potential vorticity equation becomes the familiar

$$(U(y) - c)\left(\frac{d^2A}{dy^2} - k^2A\right) + (\beta - U_{yy})A = 0. \quad (2)$$

Particular attention is focused on solutions to this equation with complex c.

The solution of (2) is made difficult by the possible presence of critical layers, where $c = U(y_c)$, within the flow. If the disturbance is growing, so that $c_i \neq 0$, the problem is non-singular on the real line and has a well-behaved solution. If the flow velocity U changes continuously with y, the only allowed neutral modes must have phase speeds either outside the range of the flow speed or equal to the flow speed where the potential vorticity-gradient vanishes (Kuo, 1949).

In order to avoid problems associated with critical layers, Rayleigh (1879) introduced a way of approximating flow profiles (with $\beta = 0$) which significantly simplified the finding of solutions. Rather than allow the flow to vary continuously in y, with isolated zeros of the vorticity gradient, he required that U_{yy} vanish everywhere *except* at isolated points, by approximating the flow with straight lines, $U_{yy} = 0$. This effectively compresses non-zero U_{yy} into delta functions at points where the straight lines meet.

This method can be extended to the β-plane by approximating the flow as

$$U = a$$

or

$$\beta - U_{yy} = 0, \quad (3)$$

where a is a constant. Thus, the potential vorticity gradient does not vanish everywhere but is equal to β, the planetary vorticity gradient, where U is independent of y. Solutions to (2) are then found in each separate region of the flow. Matching conditions on the pressure and normal velocity are applied at each profile break. The matching conditions, originally due to Rayleigh (1880), are that the displacement of the material (zonal) interface between the two regions of the flow be the same in both regions on either side of the interface, and that the tangential pressure gradient at the interface be given equally on both sides of the interface. If the profile break occurs at $y = 0$ for instance, the matching conditions are

$$\left[\frac{A(y)}{U - c}\right]_0 = 0, \quad (4)$$

$$\left[(U - c)\frac{dA}{dy} - A\frac{dU}{dy}\right]_0 = 0, \quad (5)$$

where the square brackets indicate the jump in the quantity from $y = 0 + \epsilon$ to $y = 0 - \epsilon$. Both matching conditions are unaffected by non-zero β. Application of these matching conditions and the appropriate boundary conditions to the solutions in each flow region gives the full solution and the complex phase speed $c(k)$.

3. Stability theorems

There are four useful theorems which yield information about the stability of a particular flow $U(y)$ before the detailed stability analysis is undertaken. They are well-known, so only a brief statement of each will be given here with extensions to "broken line" profiles. The first two are necessary (but not sufficient) conditions for instability. In their non-β-plane forms, they are Rayleigh's inflection point theorem (Rayleigh, 1880) and the Fjørtoft extension of this theorem (Fjørtoft, 1950). The Rayleigh theorem for homogeneous flow was extended to the β-plane by Kuo (1949). An extension of Fjørtoft's theorem to the β-plane, including stratification, was made by Pedlosky (1964). These two theorems in their normal mode, β-plane form, for unstratified flow, are

$$c_i \int_{-H}^{H} dy \frac{|A|^2}{|U - c|^2}\frac{\partial Q}{\partial y} = 0, \quad (6)$$

$$\int_{-H}^{H} dy \frac{|A|^2}{|U - c|^2} U\frac{\partial Q}{\partial y} > 0, \quad (7)$$

where $\partial Q/\partial y = (\beta - U_{yy})$. The integrals are over the domain of the flow $(-H, H)$, where H can be extended to infinity. The first theorem states that, if the growth rate of the perturbation is to be non-zero, the potential vorticity gradient $(\beta - U_{yy})$ must change sign somewhere in the flow. The second theorem says that the product $U(\beta - U_{yy})$ must be positive somewhere in the flow. [Taking the two theorems together, $(U - a)(\beta - U_{yy})$ must be positive somewhere for instability to be possible, where a is any constant.]

When the flow $U(y)$ or its derivative dU/dy are discontinuous, there are slight changes in the necessary conditions (6) and (7). The potential vorticity equation (2) is multiplied by $A^*/(U - c)$ and integrated over the entire y domain. The real and imaginary parts are separated to give the two necessary conditions for instability. For example, if there is a simple discontinuity in $U(y)$ or its derivative at $y = y_0$, the integrated equation is

$$-[A^*A']_{y_0} + \int_{-H}^{y_{0-}} dy\left\{-|A'|^2 - k^2|A|^2 + \frac{|A|^2}{U - c}\frac{\partial Q}{\partial y}\right\} + \int_{y_{0+}}^{H} dy\left\{-|A'|^2 - k^2|A|^2 + \frac{|A|^2}{U - c}\frac{\partial Q}{\partial y}\right\} = 0, \quad (8)$$

where $\partial Q/\partial y = \beta - U_{yy}$ and where the square brackets

denote the jump in the bracketed quantity across y_0. Primes denote differentiation with respect to y. Evaluation of the jump using the matching conditions (4) and (5) yields

$$-[A^*A']_{y_0} = A^*_- A'_- \frac{U_+ - c^*}{U_- - c^*}\left\{\frac{U_- - c^*}{U_+ - c^*} - \frac{U_- - c}{U_+ - c}\right\} + |A|^2 \frac{U_+ - c}{U_- - c}\left\{\frac{U'_-}{U_+ - c} - \frac{U'_+}{U_- - c}\right\}, \quad (9)$$

where the subscripts (−) and (+) indicate evaluation of the function on the southern and northern sides of the profile breaks, respectively. If, as in many cases of interest here, we have $U_+ = U_-$ with a discontinuity in dU/dy across the break, this expression becomes

$$-[A^*A']_{y_0} = \frac{|A|^2}{U - c}(U'_- - U'_+), \quad (10)$$

where U is the velocity at the break. This can be rewritten in delta-function form:

$$-[A^*A']_{y_0} = \int_{-H}^{+H} \frac{|A|^2}{U - c}(U'_- - U'_+)\delta(y - y_0)dy. \quad (11)$$

The potential vorticity gradient is generalized to

$$\frac{\partial \hat{Q}}{\partial y} = \frac{\partial Q}{\partial y} + (U'_- - U'_+)\delta(y - y_0), \quad (12)$$

where $\partial Q/\partial y$ is the well-behaved part of the potential vorticity gradient in the regions between profile breaks and $(U'_- - U'_+)\delta(y - y_0)$ is a delta function contribution to the potential vorticity gradient due to the profile breaks. The integrated potential vorticity equation (8) is

$$-\int_{-H}^{y_{0-}} dy\{|A'|^2 + k^2|A|^2\}dy - \int_{y_{0+}}^{H} dy\{|A'|^2 + k^2|A|^2\} + \int_{-H}^{+H} \frac{|A|^2}{U - c}\frac{\partial \hat{Q}}{\partial y}dy = 0. \quad (13)$$

The imaginary part of this equation gives the first necessary condition for instability:

$$c_i \int_{-H}^{+H} \frac{|A|^2}{|U - c|^2}\frac{\partial \hat{Q}}{\partial y} = 0. \quad (14)$$

If c_i is different from zero, there must be a change of sign in the effective potential vorticity gradient (12). The second necessary condition is obtained from the real part of (13). It is

$$\int_{-H}^{+H} \frac{|A|^2}{|U - c|^2}(U - c_r)\frac{\partial \hat{Q}}{\partial y}dy = \int_{-H}^{y_{0-}} |A'|^2 dy + \int_{y_{0+}}^{H} |A'|^2 dy + \int_{-H}^{H} k^2|A|^2 dy > 0. \quad (15)$$

Thus, if $(U - c_r)\partial Q/\partial y + (U'_- - U'_+)\delta(y - y_0)$ is everywhere negative, the flow must be stable.

When the flow $U(y)$ is itself discontinuous, the first derivative dU/dy at profile breaks can be represented by a delta function. The potential vorticity gradient at the profile breaks is dominated by $(-U_{yy})$, which looks like a delta-function derivative. I have not found a simple statement of the necessary conditions for this case.

Because the potential vorticity gradient is single-signed or zero everywhere in the fluid except at isolated points where it has a delta-function character, the necessary conditions for instability are satisfied only if the delta function is of the opposite sign to β. This feature is similar to that in Eady's (1949) baroclinic instability problem in which satisfaction of the necessary conditions for instability depends on delta-function contributions to the potential vorticity gradient at the upper and lower boundaries.

A third theorem, which places bounds on the phase speed and growth rate of the perturbations, is the semi-circle theorem, derived in its non-β-plane form by Howard (1961) and extended to the β-plane by Pedlosky (1964). A fourth theorem, applicable only when β is zero, is Howard's inflection-point theorem (1964). For each inflection point ($U_{yy} = 0$) there is one neutral mode with contiguous unstable solutions. This theorem has not been extended to the β-plane: it is clear from the work of Howard and Drazin (1964) and Dickinson and Clare (1973) that additional modes appear as soon as β is non-zero. The added modes appear, from the present work, to arise when the latitudinal structure of the eigenfunctions can be wavelike.

4. Radiation conditions

One purpose of this work is to explore the occurrence of "radiating" modes of instability. In a heuristic sense, this means seeking solutions that have their primary energy source in some well-defined region and that can propagate this energy to large distances (compared with the internal deformation radius, say) from the source. The word "radiating" usually describes a pure wave, say of the form $e^{ly}e^{ikx}$, where k is real and l is imaginary. When l is purely real, the solution is "trapped". When the phase speed c is complex, so that the wave is growing, the y-wavenumber is also complex. The solution is then wavelike with an evanescent envelope in y, because the *source* of energy for the wave is localized in space (at the region of horizontal shear for these barotropic instabilities). Since the disturbance is growing in time, at any time after the onset of instability, there will be a spatially decaying disturbance outside the jet, because it takes a finite time for the (initially small) disturbance to reach a point far from the jet. There-

fore, any growing wave will not look like a purely "radiating" disturbance away from the source of energy. Neutral solutions, on the other hand, will enjoy the distinction of being either purely wave-like (Rossby waves) or purely evanescent in the y-direction. The growing waves can be identified as radiating or trapped by the structure of the contiguous neutral mode, which will be either purely wave-like or purely evanescent. We identify unstable waves that neighbor neutral Rossby waves as "radiating". These unstable, radiating waves look *nearly* like Rossby waves except that they have slowly decaying envelopes imposed on the wave-like structure in y.

The definition of radiation can be quantified. If the disturbance is of the form

$$e^{i(kx+l_i y-kc_r t)}e^{-l_r y+kc_i t}$$

north of the energy source, the envelope of the disturbance moves out at the rate kc_i/l_r. As an example, look at a single unstable wave that satisfies the barotropic Rossby-wave dispersion relation in the far-field, but has complex phase speed and y-wavenumber. Its dispersion relation is

$$c_r + ic_i = U - \frac{\beta(l_i^2 - l_r^2 + k^2)}{|k^2 + l^2|^2} + i\frac{2\beta l_i l_r}{|k^2 + l^2|^2}. \quad (16)$$

Thus,

$$\frac{kc_i}{l_r} = \frac{2\beta k l_i}{|k^2 + l^2|^2}. \quad (17)$$

The ratio kc_i/l_r is the meridional group velocity: it approaches a non-zero constant as $c_i \to 0$ if the disturbance in the far-field is really a Rossby wave. If, however, this ratio approaches zero as $c_i \to 0$, the disturbance is trapped since the decay scale $(l_r)^{-1}$ remains non-zero. (Some "radiating" solutions are actually found that have $l_i \to 0$ as $c_i \to 0$, but contiguous, slightly unstable waves clearly have large decay scales and wave-like behavior in y.)

One is tempted to define a radiating instability as one that *looks* wavy in y. In fact, this is an acceptable criterion. Again, considering a barotropic Rossby wave, the y-wavenumber can be written as

$$l_i + il_r = \frac{\beta}{U - c_r - ic_i} - k^2.$$

If, as $c_i \to 0$, $(U - c_r)$ is positive and k^2 is small, the radicand is positive and l_r tends to zero. The resulting disturbance is a Rossby wave with y-wavenumber l_i. If, as $c_i \to 0$, either $(U - c_r)$ is negative *or* $(U - c_r)$ is positive and k^2 is large, the radicand is negative so that l_i tends to zero and the disturbance is trapped. Thus, if as $c_i \to 0$,

$$\left.\begin{aligned} \frac{l_i}{l_r} &\to 0, \text{ trapped disturbance} \\ \frac{l_i}{l_r} &\to \infty, \text{ radiating disturbance} \end{aligned}\right\}. \quad (18)$$

Visually, this is a measure of how "wiggly" the eigenfunction appears as $c_i \to 0$. If, as $c_i \to 0$, there are more and more oscillations before the disturbance decays away in y, the mode is radiating. Also, when $l_r = l_i$, we have

$$\frac{\beta(U - c_r)}{|U - c|^2} - k^2 = 0.$$

If the wave is not growing, and if $c_i = 0$, waves with

$$k^2 < \frac{\beta(U - c_r)}{|U - c_r|^2}$$

are purely wave-like in y, while waves with

$$k^2 > \frac{\beta(U - c_r)}{|U - c_r|^2}$$

are evanescent in y. The transition from waviness to evanescence as a function of k persists when c_i is non-zero. The criterion, $l_r = l_i$, will be used to distinguish between unstable modes that are more wave-like (and less trapped) and those that are more evanescent.

Under what circumstances will a mode be radiating away from the energy source? The first obvious requirement for radiating disturbances is that the flow in the irradiated region be capable of supporting waves. This means that there must be a potential vorticity gradient there. In addition, the phase speed condition (McIntyre and Weissman, 1978) must be satisfied: if a forced disturbance is to radiate, the phase speed and x-wavenumber of the forcing (in this case, the unstable wave) must match the phase speed and x-wavenumber of a "free" wave (essentially a Rossby wave in this case). From the semi-circle theorem, we can put limits on the allowed phase speed of an unstable wave. From the Rossby-wave dispersion relation in the outer-field, the range of Rossby-wave phase speeds in the outer-field is known. For the phase speed condition to be met, the instability phase speed must be westward with respect to the flow speed in the radiation region since Rossby waves have only westward phase speeds. This means that either a shear flow with $U_\infty \neq U_{-\infty}$ or a westward jet might radiate, while the possibilities for radiation from an eastward jet are much more restricted.

5. Shear layer instability

In this and the next section, specific results will be obtained for several velocity profiles. "Shear" layers, defined as flows with different velocities at $+\infty$ and

$-\infty$ or at the northern and southern walls (Howard and Drazin, 1964), are discussed in this section. "Jet" profiles, where the flow is the same at the outer boundaries, are discussed in section 6.

a. Shear layer with a discontinuity in U(y)

The simplest shear flow is the vortex sheet, which has a single discontinuity in $U(y)$ at, say, $y = 0$. The non-rotating (or equally, f-plane) case was discussed by Rayleigh (1879). The case with non-zero β was discussed by Howard and Drazin (1964). The necessary conditions for instability of the vortex sheet are satisfied since the potential vorticity gradient changes sign because of its double delta function (arising from U_{yy}) at $y = 0$. The solution, subject to the boundedness condition at $y = \pm\infty$, is

$$A = \begin{cases} e^{-l_I y}, & y > 0 \\ e^{l_{II} y}, & y < 0, \end{cases} \tag{19}$$

where

$$l_I = \left(k^2 + \frac{\beta}{c-1}\right)^{1/2}, \quad l_{II} = \left(k^2 + \frac{\beta}{c+1}\right)^{1/2}. \tag{20}$$

When c is complex, l_I and l_{II} are chosen to have positive real parts to satisfy the boundedness condition on the eigenfunctions at infinity. When c is real, the l's are purely real or purely imaginary. If real, they must be positive. If imaginary, the branch of l is chosen that has outward group velocity, $\partial c/\partial l$.

The dispersion relation for non-zero β was found by Howard and Drazin (1964), using the matching conditions (4) and (5):

$$c(c^2 + 1) + \frac{\beta}{4k^2}(3c^2 + 1) = 0. \tag{21}$$

There are three roots, one of them real (neutral) and the other two complex conjugates, as found by Howard and Drazin (1964). The complex roots are the unstable (growing and decaying) modes which exist for *all* β and k because 1) no β is large enough to cause the potential vorticity gradient to be of a single sign and 2) even the shortest waves sense the change in sign of $\beta - U_{yy}$, since U_{yy} has both signs right at the profile break. As $\beta k^{-2} \to 0$, $c \to \pm iU_0$. As $\beta k^{-2} \to \infty$, $c \to \pm iU_0 3^{-1/2}$. The dispersion relation is plotted in Fig. 1, showing both c_i as a function of c_r and c_i and c_r as functions of k. The phase speed depends only on the ratio βk^{-2}, so the roots for all β's follow the same curve in the $c_r - c_i$ plane. The retarding effect of β on the phase speed c_r is clearly seen at intermediate wavelengths.

What is the structure of the eigenfunctions? From (20), with $b \equiv \beta k^{-2}$,

$$\frac{l_I^2}{k^2} = 1 + \frac{b}{|c-1|^2}(-1 + c_r - ic_i),$$

$$\frac{l_{II}^2}{k^2} = 1 + \frac{b}{|c+1|^2}(1 + c_r - ic_i).$$

As β becomes large and $b \to \infty$, so that $c \to \pm iU_0 3^{-1/2}$,

$$\frac{l_I^2}{k^2} \to 3^{-1/2}\frac{2b}{|c-1|^2}e^{-i5\pi/6}, \quad \frac{l_{II}^2}{k^2} \to 3^{-1/2}\frac{2b}{|c+1|^2}e^{-i\pi/6}$$

and $l_I k^{-1}$ is proportional to $e^{-i5\pi/12} = (.26 - .97i)$ while $l_{II}k^{-1}$ is proportional to $e^{-i\pi/12} = (.97 - .26i)$. In the northern half of the profile where the flow is more eastward, the eigenfunction is *more* oscillatory and decays more slowly than in the southern half. (To the north, the instability phase speeds are always less than the flow speed, so the long waves satisfy the phase-speed condition and look like Rossby waves with complex phase speed and complex y-wavenumber.) However, because the growth rates of disturbances are non-zero for all choices of β and k, there is always a pronounced, meridionally-decaying envelope.

b. Shear profile with discontinuities in dU/dy.

The vortex sheet results of the previous section explain some of the behavior of the unstable modes of a shear profile, but since any realistic shear zone

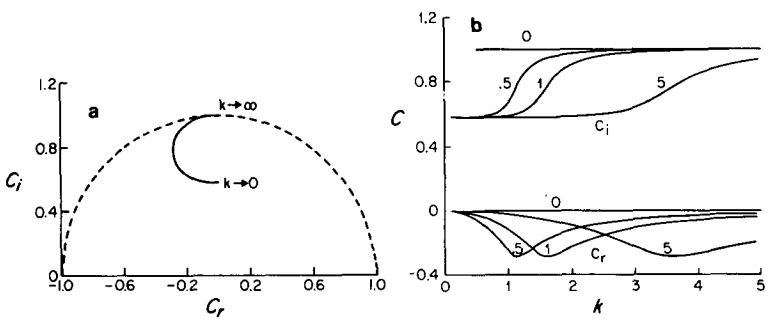

FIG. 1. Vortex sheet dispersion relation: (a) $c_i(c_r)$ and (b) $c_r(k)$ and $c_i(k)$. At $\beta = 0$, c_r and c_i must fall inside the dashed curve according to the semi-circle theorem.

has non-zero width, the results strictly apply only to the behavior of long waves which see a shear zone as a discontinuity in $U(y)$. In a realistic flow where the shear zone has non-zero width, the short waves should be stabilized with maximum growth rate at an intermediate wavelength. A smoothly varying flow will also be stable if β is large enough to make the potential vorticity gradient single-signed everywhere.

The flow is approximated using the method of Section 2 in which the potential vorticity gradient is zero or uniform in discrete regions of the flow. The velocities are

$$\left.\begin{aligned} U_{\mathrm{I}} &= -1 \\ U_{\mathrm{II}} &= -\frac{\beta}{2} - y + \frac{\beta}{2}y^2 \\ U_{\mathrm{III}} &= 1 \end{aligned}\right\}. \tag{22}$$

The potential vorticity gradient is β in Regions I and III, so waves can be supported there when β is non-zero. The velocity profile and a schematic of its potential vorticity gradient are shown in Fig. 2 for two values of β. Change in sign of the potential vorticity gradient occurs only because of delta function contributions to $-U_{yy}$ at $y = \pm 1$, since it is positive or zero everywhere in Regions I, II and III. As β increases, the velocity profile changes in Region II until $(\beta - U_{yy})$ is positive everywhere. At this β $(=\beta_c)$, the flow must be stable, and hence this patched profile mimics the β-stabilization that occurs in smoothly-varying flows. This can be seen in Fig. 2 where $U(y)$ and $\partial\hat{Q}/\partial y$ are shown for supercritical and subcritical β. The maximum β for which instability is possible is $\beta = 1$, from (22).

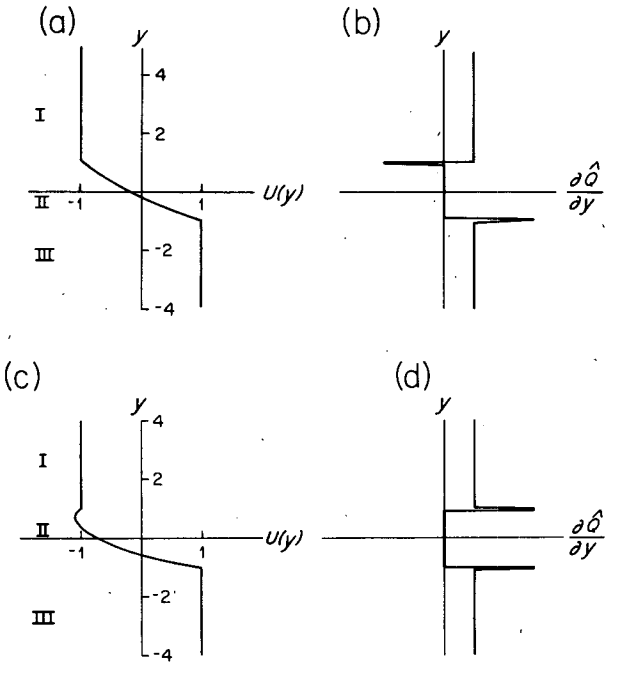

FIG. 2. Shear layer: $U(y)$ and $\partial\hat{Q}/\partial y$ for two choices of β. (a) and (b): $\beta = 0.5$ (supercritical); (c) and (d): $\beta = 1.5$ (subcritical).

The solution to the potential vorticity equation, subject to boundedness conditions at infinity, is

$$\left.\begin{aligned} A_{\mathrm{I}} &= e^{-ly} \\ A_{\mathrm{II}} &= a_1 e^{ky} + a_2 e^{-ky} \\ A_{\mathrm{III}} &= de^{l_{\mathrm{III}}y} \end{aligned}\right\}, \tag{23}$$

where $l_{\mathrm{I}}^2 = k^2 + \dfrac{\beta}{1+c}$ and $l_{\mathrm{III}}^2 = k^2 - \dfrac{\beta}{1-c}$, just as in the previous example. The dispersion relation obtained from the matching conditions is

$$\begin{aligned} &e^{-4k}\left\{\left[1 - \left(1 + \frac{b}{1+c}\right)^{1/2}\right](1+c) + \frac{1}{k}(1-\beta)\right\} \\ &\times \left\{\left[1 - \left(1 + \frac{b}{c-1}\right)^{1/2}\right](1-c) + \frac{1}{k}(1+\beta)\right\} \\ &- \left\{-\left[1 + \left(1 + \frac{b}{1+c}\right)^{1/2}\right](1+c) + \frac{1}{k}(1-\beta)\right\} \\ &\times \left\{-\left[1 + \left(1 + \frac{b}{c-1}\right)^{1/2}\right](1-c) + \frac{1}{k}(1+\beta)\right\} = 0, \end{aligned} \tag{24}$$

where $b \equiv \beta k^{-2}$.

The variable parameters are β and k. Various limits of the dispersion relation can be examined before solving it numerically:

1) $k \to 0$, β fixed: the dispersion relation is

$$2\beta^{1/2}\{\beta + c + \beta(c^2-1)^{1/2} + [\beta(c-1)]^{1/2}\} + (1+c)^{3/2} + (c-1)^{3/2} = 0.$$

As $\beta \to 0$, $c \to \pm i3^{-1/2}$, which is the long-wave limit of the vortex sheet instability. As $\beta \to \infty$, $c \to -(\beta k^{-2})$ [with $k = \mathrm{O}(1/\beta)$].

2) $k \to \infty$, β fixed: $c = \pm 1$.

3) $\beta \to 0$, k fixed:

$$c = \pm\left[1 - \frac{1}{k} + (2k)^{-2}(1 - e^{-4k})\right]^{1/2}.$$

As $k \to 0$, $c = \pm i$, the short-wave limit for the vortex sheet. As $k \to \infty$, $c = \pm 1$.

4) $\beta \to \infty$, k fixed: $c = \beta(1 - 2k)$. Additional informative limits are obtained by letting the length scale L approach zero and infinity, with $\beta = \beta_0 L^2 U_0^{-1}$ and $k = k^* L$.

5) $L \to 0$: $(l_{\mathrm{I}}k^{-1})(1+c)^2 + (l_{\mathrm{III}}k^{-1})(1-c)^2 = 0$, the vortex sheet dispersion relation.

6) $L \to \infty$: $c \to -\beta/2k$.

One other limit that reveals the retarding effect of β is

7) $k \to \infty$, $\beta = O(k)$: $c = \pm 1 - \beta/2k$.

The long-wave limits are identical to the vortex sheet results: when β approaches zero faster than k, the limit $c = \pm i$ is obtained, while when β approaches zero more slowly than k, the limit is $c = \pm i 3^{-1/2}$. The short-wave limit in all cases is a stable solution, with $c = \pm 1$. For the limit where L increases to ∞, the flow appears to be an infinitely wide Couette flow to the short waves, which are thus stable.

These limits delineate the results to be expected from the dispersion relation. The dispersion relation (24) was solved numerically using the secant method with complex arithmetic to find the roots $c(k)$ for given β and k. Fig. 3 is the neutral stability diagram in the $\beta - k$ plane for this profile. The dashed curve is the locus $\mathrm{Re}(l_{III}) = \mathrm{Im}(l_{III})$. The short waves are more trapped and less wave-like in region III than the long waves. The stability cutoffs were found up to $\beta = 0.95$: extrapolating the growth rates to the β where $c_i = 0$, the long waves are all unstable up to $\beta = 1.0$ and the short waves are probably also unstable up to 1.0, with a cusp in the stability diagram there (so that there is a single short-wave neutral mode at $\beta = 1$). At high β, there are two separate ranges of unstable wavenumbers. These are two separate modes

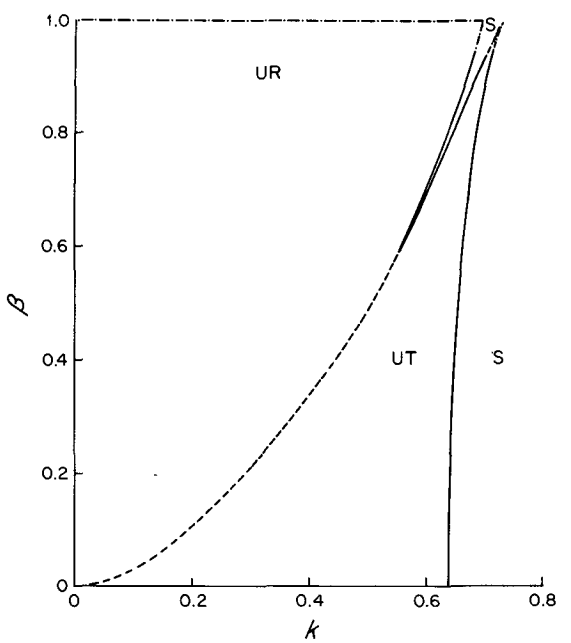

FIG. 3. Shear layer stability diagram. $c_i = 0$ along the solid curves. The dotted curve is where $\mathrm{Re}(l_{II}) = \mathrm{Im}(l_{II})$ and corresponds to the transition from radiating long waves to trapped short waves. The dot-dashed curves are extrapolated stability boundaries, $c_i = 0$. S means "stable", UT means "unstable, trapped" and UR means "unstable, radiating".

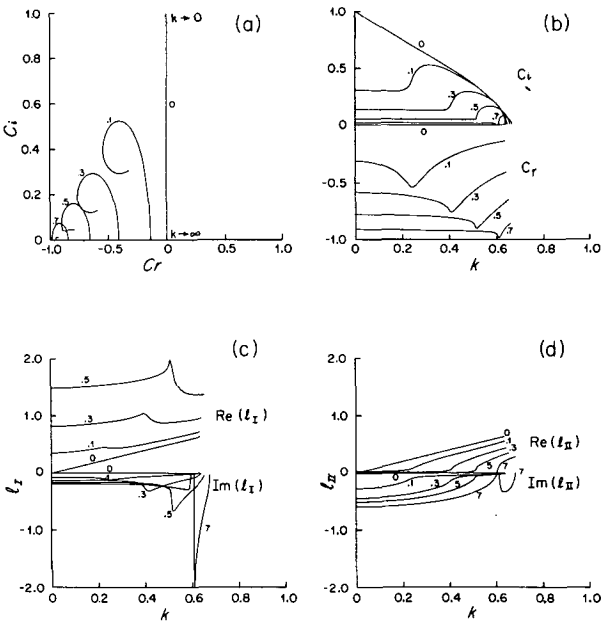

FIG. 4. Shear layer dispersion relation for $\beta = 0, .1, .3, .5, .7$. (a) $c_i(c_r)$, (b) $c_r(k)$ and $c_i(k)$, (c) $\ell_I(k)$, and (d) $\ell_{III}(k)$. The northern and southern meridional decay scales are $[\mathrm{Re}(\ell_I)]^{-1}$ and $[\mathrm{Re}(\ell_{III})]^{-1}$ respectively.

which coalesce as β decreases, and are similar to the two separate modes found by Dickinson and Clare (1973) for the hyperbolic tangent shear layer. The flow is stable for all β's greater than 1, the cut-off required by the necessary condition for instability: the necessary condition is sufficient for this profile.

Figs. 4a, b show c_i as a function of c_r and c as a function of k for several choices of β. At $\beta = 0$, the well known result for a Rayleigh broken-line profile with a non-zero width shear zone is obtained. There is a dramatic change in the long-wave behavior when even a small amount of β is introduced. The growth rate drops dramatically and the phase speed is retarded (made more westward). There is a cusp in the real phase speed and a sudden change in the imaginary phase speed at intermediate k: both are nearly constant at low k. As β increases, a tiny intermediate range of wavenumbers is stabilized, separating the long- and short-wave behavior. As β nears the cutoff of 1, the growth rate approaches 0 and the phase speed of all unstable waves approaches -1, the minimum flow speed.

The structures of the long- and short-wave modes are quite different. Figs. 4c, d show the real and imaginary parts of l_I and l_{III} for several β's. The decay scales are given by $[\mathrm{Re}(l_I)]^{-1}$ and $[\mathrm{Re}(l_{III})]^{-1}$ and the y-wavenumbers by $\mathrm{Im}(l_I)$ and $\mathrm{Im}(l_{III})$. When $\mathrm{Re}(l)$ is small and $\mathrm{Im}(l)$ is large, the disturbances radiate. On the northern side of the profile where $l = l_I$, the disturbances are always trapped. On the southern side

where $l = l_{III}$, the long waves radiate with a clear transition to trapped behavior as k increases.

Eigenfunctions at $\beta = 0.5$ are shown in Fig. 5, showing the difference in trapping scales of the radiating and trapped modes. Both the short- and long-wave modes are evanescent on the northern side of the shear layer where the flow is easterly and the phase speed condition cannot be satisfied. On the southern side of the shear layer, the short-wave mode is trapped and the long-wave mode is radiating even though the phase speeds of both modes are westward with respect to the flow speed. The difference in behavior is due to satisfaction (or lack thereof) of the phase speed condition. The Rossby-wave dispersion relation with a mean flow of $U = 1$, for $\beta = 0.5$, is plotted in Fig. 6 for two extreme y-wavenumbers. Also shown in Fig. 6 are the phase speeds of the instabilities at $\beta = .5$: the change in behavior from radiating to trapped occurs where the instability dispersion relation intersects the Rossby-wave dispersion relation near $l = 0$. The phase speed condition is satisfied on the long-wave side of this intersection, while the shorter waves cannot match any Rossby waves in the far-field.

Thus, for this simple shear profile there are radiating modes when the range of instability phase speeds allowed by the semi-circle theorem overlaps the range of Rossby-wave phase speeds in the far-field. These can be thought of as destabilized Rossby waves rather than as inherent instabilities of the shear layer. Although there are many Rossby waves at each x-wavenumber, $0 < k < \infty$, that potentially could be destabilized, the short waves are stable and only one Rossby wave at each long wavelength is destabilized. The short-wave cutoff is presumably due to lack of penetration into the shear layer as k increases (23).

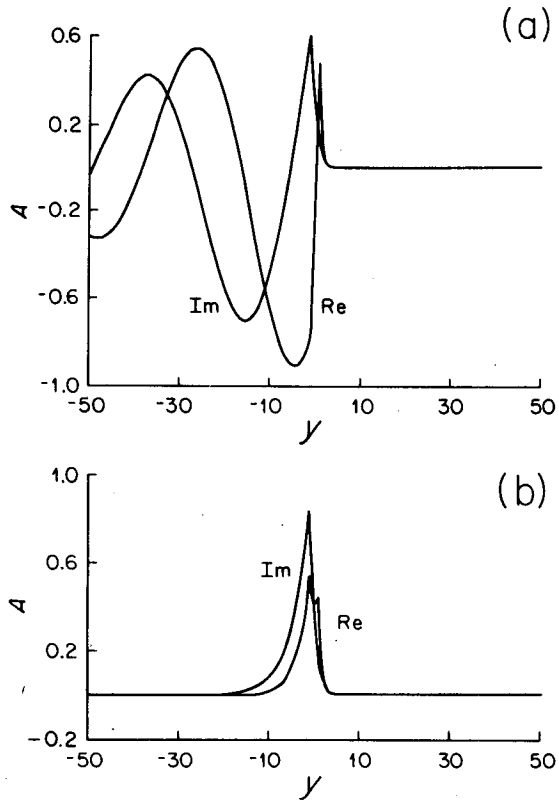

FIG. 5. Shear layer eigenfunction amplitude, $A(y)$, at $\beta = 0.5$ for (a) $k = 0.5$ (radiating mode) and (b) $k = 0.6$ (trapped mode).

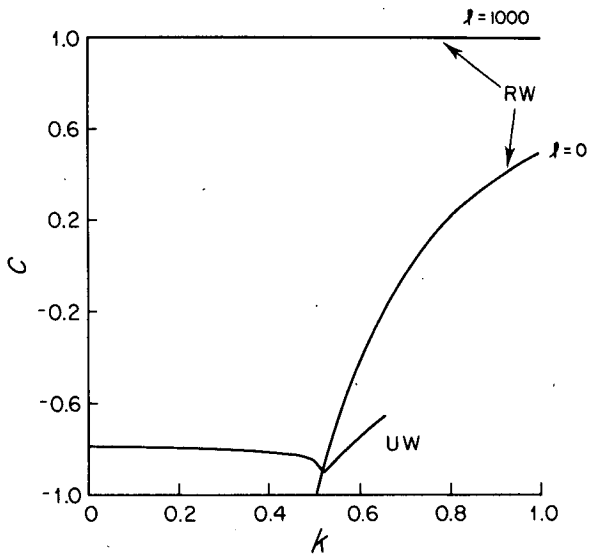

FIG. 6. Phase speed of barotropic Rossby waves (RW) and shear layer instabilities (UW) at $\beta = 0.5$. The barotropic Rossby wave phase speed in a mean flow $U = 1$ is shown for y-wavenumbers 0 and 1000.

Comparison of the results from this profile with the results of Howard and Drazin (1964) and Dickinson and Clare (1973) for the shear profile, $U(y) = \tanh y$, indicates how well the broken profile represents a smoothly varying flow. Howard and Drazin (1964) found the trapped, unstable mode of the shear flow and predicted an additional unstable, long-wave, low-β mode. Dickinson and Clare (1973) found the unstable modes of the hyperbolic-tangent profile numerically. At low β and k, there are two distinct modes of instability, overlapping in wavenumber. The first mode is strongly trapped to the region of maximum horizontal shear, corresponding to Howard and Drazin's (1964) main mode, while the second mode is "radiating" with much slower meridional decay, corresponding to Howard and Drazin's additional mode. Because the stability diagram is complicated by the radiating mode at low β and k, Dickinson and Clare did not draw the completed stability diagram for low wavenumbers. At higher β, the two modes do not overlap in wavenumber but the growth rate of the radiating mode is very small. Large β stabilizes the flow altogether.

The unstable modes of the pieced shear layer are very similar to the unstable modes of the hyperbolic-tangent flow in that there are trapped and radiating instabilities with roughly similar neutral curves. The main differences are that 1) at low β, where the hyperbolic-tangent flow has two separate modes overlapping in wavenumber, the present model has a single mode which is a combination of the two hyperbolic-tangent modes, without the lower growth rate parts of the overlapping modes, and 2) where the oscillatory mode for the hyperbolic-tangent profile is limited to a small range of β and k, the oscillatory mode for the shear layer occurs for all values of β up to the cutoff dictated by the necessary condition for instability. The first difference suggests that mode coalescence occurs more readily for "broken line" profiles than for continuous profiles. The second difference may not be a difference at all: the "neutral" modes of the hyperbolic-tangent profile were determined numerically and were defined to have a certain, small c_i. The true neutral curve for the radiating mode may really be similar to the neutral curve found here, extending to the maximum β allowed by the necessary condition for instability.

The close correspondence of the present results to those of Dickinson and Clare (1973) is important to note since it was not clear at the outset that this would be true. Similar results were obtained because both profiles were 1) monotonically sheared, 2) on the β-plane with the potential-vorticity gradient in the far-field essentially equal to β, and 3) stabilized by large β. The variation of $U(y)$ with β in the present case may seem to present intuitive difficulties, but in fact it is necessary if the flow is to be stabilized by increasing β.

6. Barotropic jets

A jet is defined as a flow that has the same velocity at $+\infty$ and $-\infty$ (Howard and Drazin, 1964). Only symmetric jets with no more than two inflection points in U are considered here. Howard's (1964) inflection-point theorem predicts two neutral modes with contiguous unstable modes at $\beta = 0$ when there are two inflection points (where $U_{yy} = 0$). The theorem does not predict the number of modes when β is non-zero and, in fact, we saw in the previous section that a new mode, associated with Rossby waves outside the shear layer, was introduced when β was non-zero. A search for unstable modes of a jet can, however, be begun at $\beta = 0$ where there will be two unstable modes. If the jet is symmetric, the two modes will be sinuous (symmetric) and varicose (antisymmetric).

The jets considered here are: (1) top-hat, eastward jet, (2) eastward jet with shear layers, and (3) westward jet with shear layers. ("Westward" jets were explored by allowing non-dimensional β to be negative.) Eastward and westward jets are considered separately because their potentials for radiation of energy in the far-field differ radically. (The energy from the horizontal shear of an eastward jet essentially "radiates" to the *inside* of the jet.)

The velocity profiles are chosen by the method explained in Section 2. Fig. 7 shows the eastward jets and a schematic of their potential vorticity gradients. The potential vorticity gradient for the top-hat jet includes a double delta function (due to U_{yy}) at the profile breaks. Because the top-hat shape is independent of β, there is no range of β for which this flow is absolutely stable by the necessary condition (14) since the potential vorticity gradient changes sign for any choice of β. The shear-layer jet differs in this respect. Its shape in the shear zones depends on β in the same way as the shear profile of the previous section. When β is large enough, the delta function for U_{yy} at the profile breaks becomes positive and the potential vorticity gradient is positive everywhere (for eastward flow). The flow then must be stable for all β larger than a critical value, β_c, which depends on the width ($D - 1$) of the shear layer.

a. *Eastward top-hat jet*

The unstable modes of the top-hat jet are well-known, although aspects of their behavior as β increases are explored here for the first time. Rayleigh (1879) first posed the problem of the top-hat jet, for the case $\beta = 0$. Howard and Drazin (1964) extended it to the β-plane, giving analytical results for the phase speed and growth rate for various limits of wavenumber and β. Flierl (1975) discussed the full behavior for varying values of βk^{-2}, although he did not completely explore the β and k parameter ranges.

When β is non-zero, the dispersion relations for the sinuous and varicose modes, obtained from the

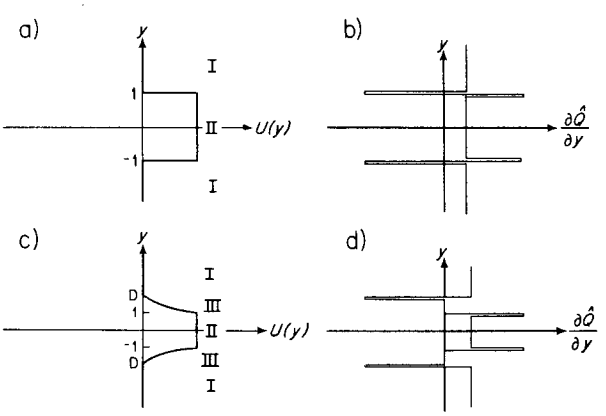

FIG. 7. Barotropic jets: (a) $U(y)$ and (b) $\partial\hat{Q}/\partial y$ for the top-hat jet. (c) $U(y)$ and (d) $\partial\hat{Q}/\partial y$ for the barotropic jet.

solution to (2) in Regions I and II and the matching conditions (4) and (5) are (Howard and Drazin, 1964):

$$\left.\begin{aligned} c_1^2 l_{\mathrm{I}} + l_{\mathrm{II}}(1-c_1)^2 \tanh l_{\mathrm{II}} &= 0 \\ c_2^2 l_{\mathrm{I}} \tanh l_{\mathrm{II}} + l_{\mathrm{II}}(1-c_2)^2 &= 0 \end{aligned}\right\}, \tag{25}$$

where

$$\left.\begin{aligned} l_{\mathrm{I}}^2 &= k^2 + \frac{\beta}{c} \\ l_{\mathrm{II}}^2 &= k^2 + \frac{\beta}{1-c} \end{aligned}\right\}. \tag{26}$$

Here c_1 corresponds to the symmetric mode and c_2 to the antisymmetric mode. The eigenfunction is

$$\left.\begin{aligned} A_{\mathrm{I}} &= e^{-l_{\mathrm{I}} y} \\ A_{\mathrm{II}} &= d(e^{l_{\mathrm{II}} y} \pm e^{-l_{\mathrm{II}} y}) \end{aligned}\right\}, \tag{27}$$

where the (+) sign is for the sinuous mode and the (−) sign for the varicose mode and

$$d \equiv \frac{c-1}{c} \times \frac{e^{-l_{\mathrm{I}}}}{e^{l_{\mathrm{II}}} \pm e^{-l_{\mathrm{II}}}}.$$

The limits of the dispersion relation as βk^{-2} and k take extreme values are given by Howard and Drazin (1964). Both the varicose and sinuous modes are unstable at very large k [where $c \to \frac{1}{2}(1 \pm i)$] and very large β [where $c \to \frac{1}{2}(1 \pm i/3^{1/2})$].

The sinuous modes of the eastward top-hat jet are unstable for ranges of β and k shown in the stability diagram of Fig. 8. Notice that the long waves are stable at low β, but that increasing β actually destabilizes the modes again. These waves will be called "β-destabilized" modes. All waves with high β and high k are unstable. A dispersion relation illustrating the β-destabilized mode and the main mode is shown in Fig. 9. In Fig. 9 the corresponding real and imaginary parts of l_{I} and l_{II} are also plotted. Both modes are trapped to the jet. They behave differently inside the jet, however: from l_{II}, we see that the β-destabilized mode is wave-like and the main mode is evanescent inside the jet. The β-destabilized mode has a cross-jet wavenumber near the neutral curve of roughly $\pi/2$ at small k.

The stability diagram for the varicose mode of the top-hat jet (Fig. 10) is similar to the diagrams for the sinuous mode (Fig. 8). Again there is a small region where the varicose mode is stable, but it is now centered at higher β. All waves are trapped to the jet. The details of the stability diagram again depend on the structure of the eigenfunctions within the jet: the β-destabilized modes are more wave-like inside the jet than the short-wave, low-β modes. Dispersion relations as functions of k for several β's are shown in Fig. 11. There is a large shift in phase speed across

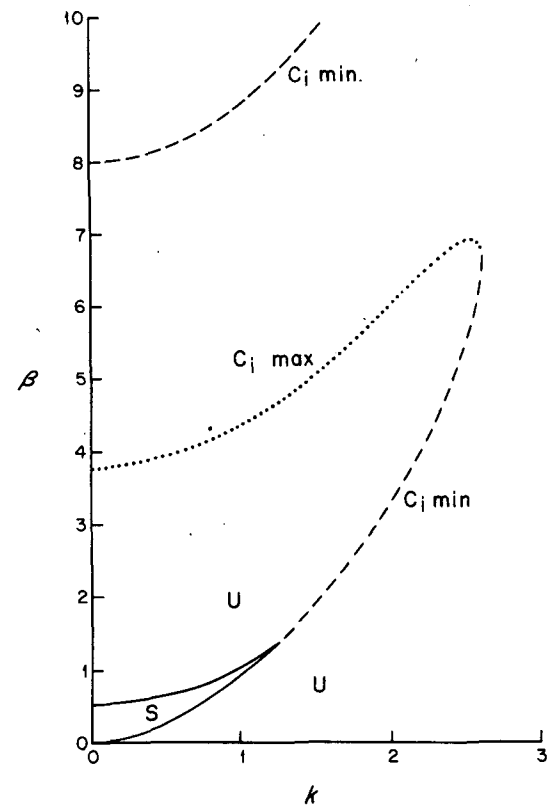

FIG. 8. Top-hat jet (sinous mode) stability diagram in the β-k plane. S means stable and U means unstable.

the stable region of the stability diagram for $\beta \geq 3$. Also shown in Fig. 11 are l_{I} and l_{II}. Outside the jet, the disturbances are trapped since $\mathrm{Re}(l_{\mathrm{I}})$ is rather large. *Inside* the jet, the eigenfunctions with small k and high β are wave-like. The y-wavelength inside the jet for these eigenfunctions is roughly π, corresponding with the lowest cross-channel, antisymmetric mode.

Thus, both the sinuous and varicose modes are stable in a small region of the $\beta - k$ plane, with a locus of minimum c_i extending to infinite β from the stable region. The stable region and curve of minimum c_i mark a transition from evanescent to radiating behavior *inside* the jet. That is, since

$$l^2 = k^2 - \frac{\beta}{1-c}$$

inside the jet, l^2 is positive or negative depending on how large k and β are if c is real. When k is large or β small, the disturbance is evanescent inside the jet. As β increases relative to k, l becomes imaginary and the disturbance is wave-like inside the jet. When c is complex, this distinction is blurred. However, the waves with high k and low β in Figs. 8 and 10 are more evanescent inside the jet than the low-k, high-

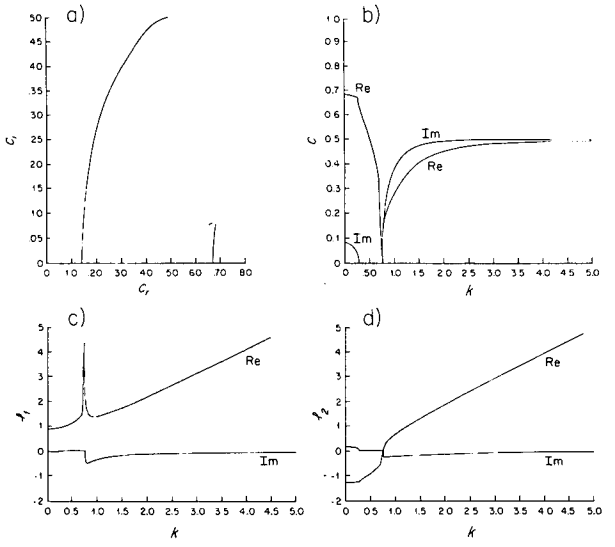

FIG. 9. Top-hat jets: sinous mode at $\beta = 0.55$. (a) $c_i(c_r)$, (b) $c_r(k)$ and $c_i(k)$, (c) $\ell_I(k)$, and (d) $\ell_{II}(k)$.

β waves. I do not have an explanation for the stability of the profile in the narrow wedge in the β-k plane.

b. *Barotropic jet*

The logical extension of the top-hat jet is a jet with horizontal shear occurring over a zone of non-zero width, as shown in Fig. 7. This profile is similar to the shear layer profile, so it can be predicted that any Rossby wave-like behavior will be confined to the more westerly part of the flow, which is the central jet in this case. Thus, the eastward jet will probably not radiate energy outside the jet. In contrast to the top-hat jet, the barotropic jet is stabilized when β is large enough to make the potential vorticity gradient single-signed, just as for the shear layer. The barotropic jet is also stable to short-wavelength perturbations, like the shear layer, since the short waves are less able to sample the full width of the shear zone (which they must do if they are to "see" the change in sign of the potential vorticity gradient.)

The profile has uniform velocity in Regions I and II and

$$U = 1 - \left(\frac{1-y}{1-D}\right) + \frac{\beta}{2}[D(1-y) - y + y^2]$$

in Region III. The potential vorticity is β in Regions I and II and zero in Region II. The length scale L^* is the half-width of the central jet, Region II. The width of the shear zone, Region III, is $(D^* - L^*)$ and its non-dimensional width is $(D - 1)$. The flow is stable when β is large enough to make dU/dy at $y = \pm D$ negative. This occurs when

$$\beta = \beta_c = \frac{2}{(D-1)^2}. \tag{28}$$

The dispersion relation derived from the matching conditions for the symmetric mode is

$$\begin{aligned} &e^{-kS}\left\{c\left[1 - \left(1 + \frac{a}{c}\right)^{1/2}\right] + \frac{1}{k}\left(\frac{1}{S} + \frac{\beta}{2}S\right)\right\} \\ &\times \left\{(1-c)\left[1 - \left(1 - \frac{a}{1-c}\right)^{1/2}\right.\right. \\ &\left.\left. \times \tanh k\left(1 - \frac{a}{1-c}\right)^{1/2}\right] + \frac{1}{k}\left(\frac{1}{S} + \frac{\beta}{2}S\right)\right\} \\ &+ e^{kS}\left\{c\left[1 + \left(1 + \frac{a}{c}\right)^{1/2}\right] - \frac{1}{k}\left(\frac{1}{S} + \frac{\beta}{2}S\right)\right\} \\ &\times \left\{-(1-c)\left[1 + \left(1 - \frac{a}{1-c}\right)^{1/2}\right.\right. \\ &\left.\left. \times \tanh k\left(1 - \frac{a}{1-c}\right)^{1/2}\right] + \frac{1}{k}\left(\frac{1}{S} + \frac{\beta}{2}S\right)\right\} = 0, \end{aligned} \tag{29}$$

where $S = (D - 1)$ and $a = \beta k^{-2}$. When $S \to 0$, the top-hat dispersion relation (24) is obtained. The flow is stable at high wavenumber since $c \to 0$, 1 as $k \to \infty$ with β fixed and $c \to -\beta S/2k$, $1 - \beta S/2k$ as $k \to \infty$ with $\beta = 0(k)$. In addition, the flow must be stable at high β because of the necessary condition for instability.

The stability diagram in the β-k plane for the sinuous mode is shown in Fig. 12 for two shear-zone widths. The β_c's for several shear-zone widths are listed as follows:

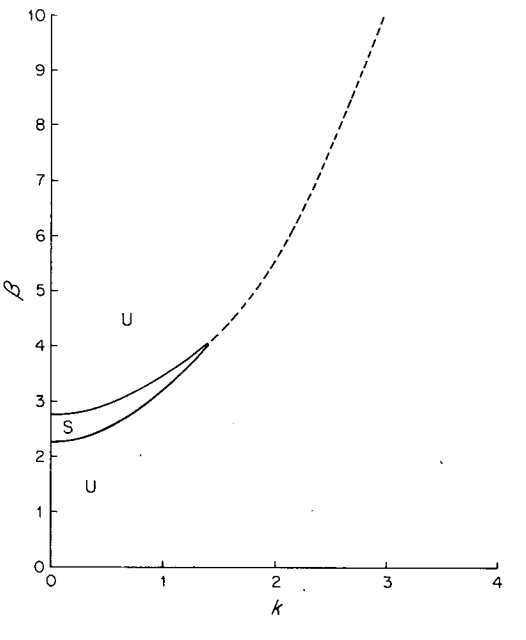

FIG. 10. Top-hat jet (varicose mode) stability diagram. The dashed curve is the locus of minimum c_i.

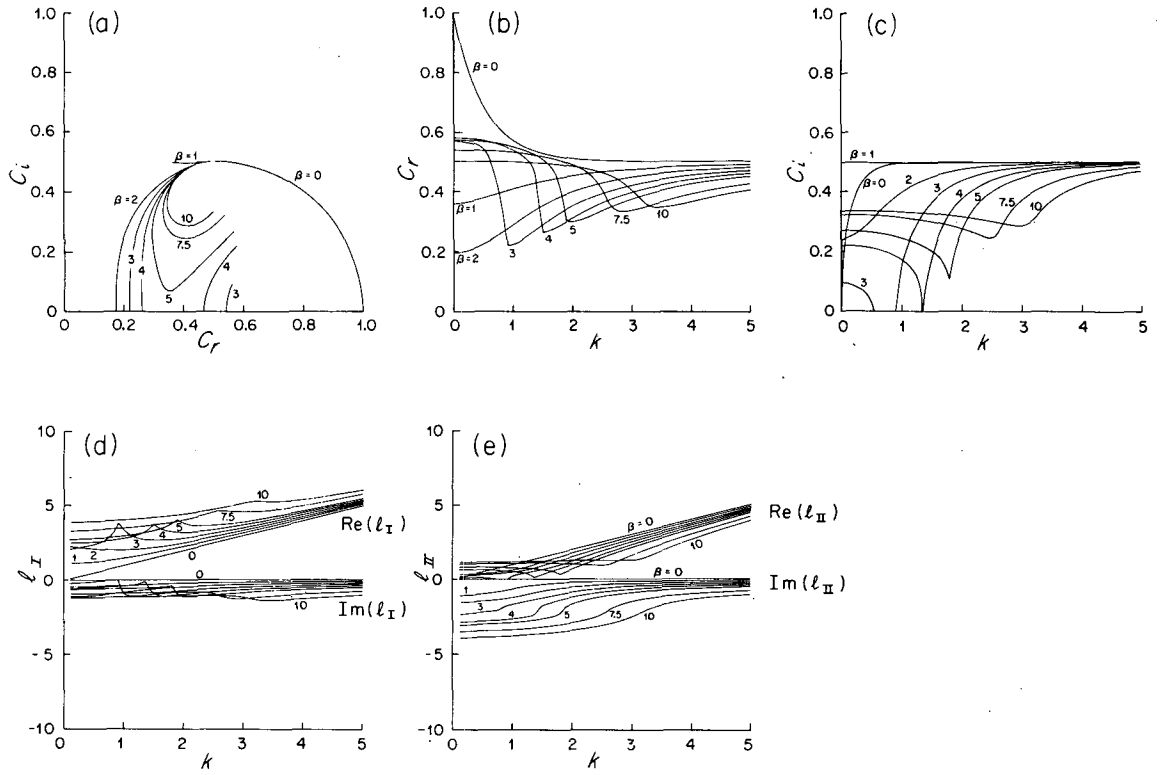

FIG. 11. Top-hat jet: varicose mode. (a) $c_i(c_r)$, (b) $c_r(k)$, (c) $c_i(k)$, (d) $\ell_I(k)$, and (e) $\ell_{II}(k)$ for the indicated values of β.

$(D-1)$	β_c
0.0	∞
0.05	800.00
0.5	8.00
0.7	4.08
1.0	2.00 .

There are three effects of increasing the shear-zone width: 1) the short-wave cutoff occurs at lower values of k; 2) as the shear zone widens, β_c decreases from ∞ for a top-hat jet to 2 for a jet with shear-zone widths equal to the central jet half-width, 3) the β-destabilized modes occur at higher β as D increases. The last two tendencies are opposing: as the shear zone widens, the β-destabilized modes disappear since β_c is decreasing while the modes occur at higher and higher β. When the shear zone narrows, there are many β-destabilized modes as β is increased to β_c at $k = 0$. As the shear zone is widened, fewer unstable modes appear until there is only one unstable mode when D is between 1.55 and 1.6. This single mode persists for all D's larger than 1.6.

The unstable regions on the stability diagram (2.6.6) all terminate in a cusp at β_c. This cusp may be an artifact of the specific choice of profile with breaks in U or dU/dy [such cusps do not appear in the stability diagram for the continuous tanh$y$ shear flow (Howard and Drazin, 1964)].

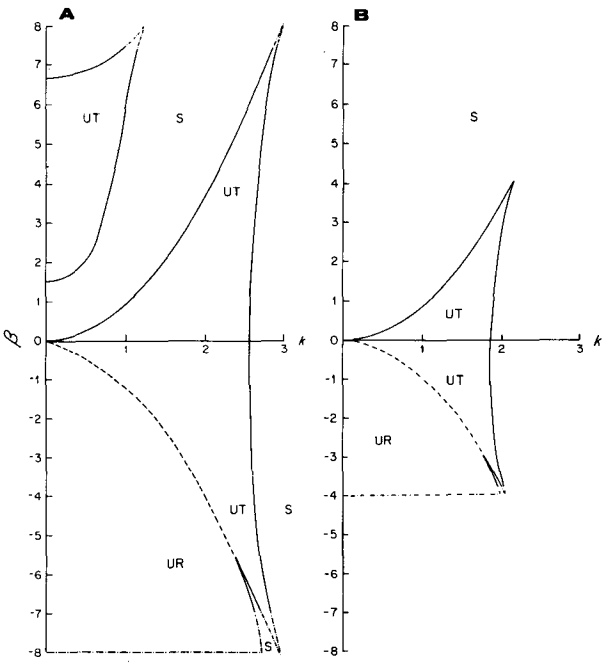

FIG. 12. Barotropic jet, sinous mode: stability diagram in the β-k plane for shear zone widths $(D-1) = 0.5$ and 0.7. "S" = stable, "UT" = unstable, trapped, "UR" = unstable, radiating. The solid curves are neutral curves and the dot-dashed curves are extrapolated neutral curves. The dashed curves are the loci Re(ℓ_I) = Im(ℓ_I).

Dispersion relations, l_I and l_{II} are shown in Fig. 13 for two values of β at $D = 1.5$. Note that increasing β tends to decrease the eastward phase speed and growth rates of the instabilities.

None of the unstable modes of the barotropic eastward jet radiate since their phase speeds are always more eastward than the flow speed outside the jet. This could not be predicted by the semi-circle theorem, since the semi-circle theorem is modified when β is non-zero to include the possibility of unstable waves with phase speeds *less* than the minimum phase speed. However, Tung (1981) showed that the neutral mode contiguous to unstable modes with phase speeds outside the range of $U(y)$ must have its phase speed *within* the range of $U(y)$. Thus, an eastward, barotropic jet can have no radiating modes.

The instabilities of westward barotropic jets radiate since their phase speeds are in the range of Rossby-wave phase speeds in the far-field. However, the barotropic jet resembles the barotropic shear layer, folded over onto itself, which had radiating solutions in the more westerly part of the flow. To look at westward jets, we simply allow $\beta = \beta_0 L^2 U^{-1}$ to be negative. The stability diagram (Fig. 12) for negative β is very similar to the shear layer stability diagram (Fig. 3). The dotted curve effectively separates radiating solutions, on the long-wave side, from trapped solutions, on the short-wave side. At large β, there is actually a range of stable waves between the radiating and trapped instabilities. The stability boundary at large β is at $\beta = \beta_c$ for both radiating and trapped solutions. While the unstable region for the trapped solutions terminates in a cusp at $\beta = \beta_c$, the radiating solutions are unstable for a wide range of low wavenumbers up to $\beta = \beta_c$. The short-wave cutoff at a given β for the radiating (long wave) mode apparently could be predicted if the neutral mode's phase speed were known since the meridional wavenumber $\mathrm{Re}(l_I)$ always appears to be zero for the neutral mode.

The dispersion relation and eigenfunctions for the westward jets are also very similar to those of the barotropic shear layer. In Fig. 14, the dispersion relation and y-dependences [$l_I(k)$, $l_{II}(k)$] are shown. The similarity to the shear-layer dispersion relation (Fig. 5) is obvious: the growth rate and phase speed of the long waves are depressed compared with those of the shorter waves. The long waves radiate outside the jet, as evidenced by the small size of $\mathrm{Re}(l_I)$ and large size

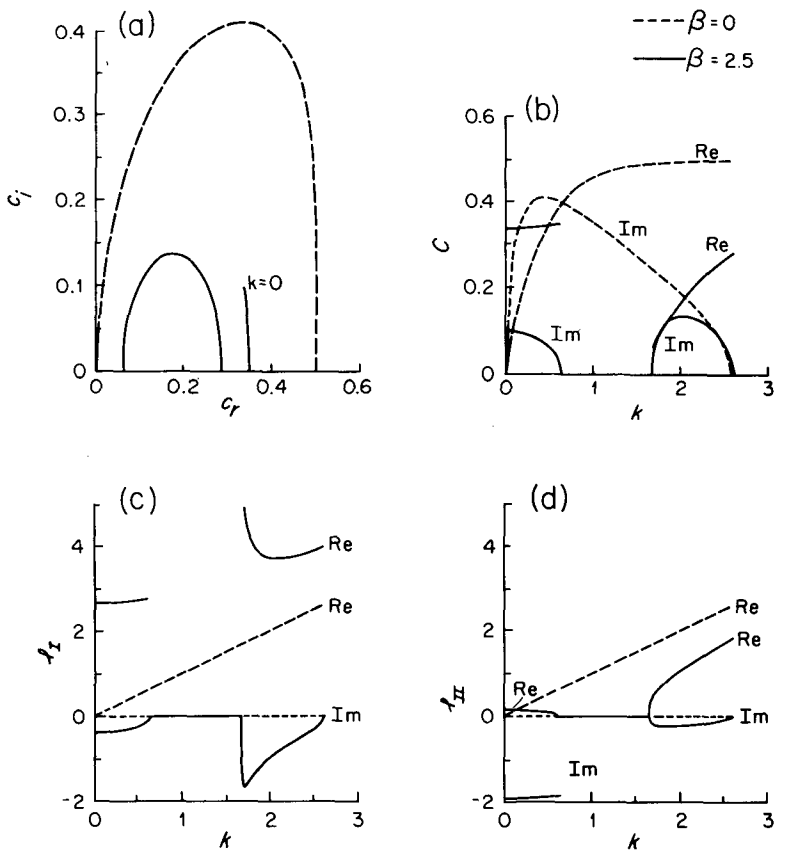

FIG. 13. Barotropic jet, sinuous mode: dispersion relations for $D = 1.5$. (a) $c_i(c_r)$, (b) $c_r(k)$ and $c_i(k)$, (c) $\ell_I(k)$ and (d) $\ell_{II}(k)$ for $\beta = 0, 2.5$.

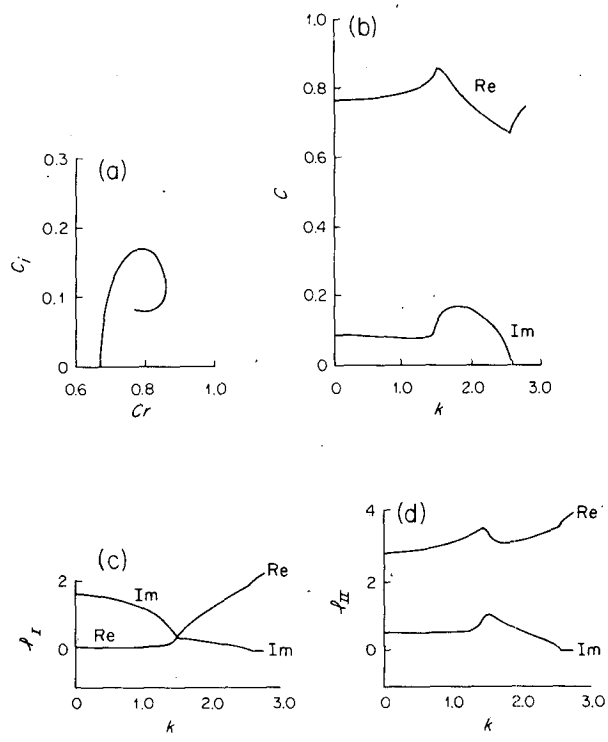

FIG. 14. Barotropic jet, sinuous mode, at $D = 1.5$ and $\beta = -2.0$: (a) $c_r(c_i)$, (b) $c_r(k)$ and $c_i(k)$, (c) $\ell_I(k)$ and (d) $\ell_{II}(k)$.

of Im(l_I). Eigenfunctions for a radiating and a trapped mode are shown in Fig. 15 (for the north side of the jet only): the difference in their behavior is striking.

7. Summary

A method for simplifying a barotropic flow profile when the ambient potential-vorticity gradient is non-zero was introduced. The results for a monotonic shear layer agree well with Dickinson and Clare's (1973) linear-stability results for the hyperbolic-tangent shear layer. Necessary conditions for instability were restated to include the effects of discontinuities in the first derivative of the basic velocity, dU/dy. Results for eastward and westward jets were also explored, assuming that these results also resemble the results for a continuous flow profile.

Because of the way the profiles with shear layers are constructed, they simulate the behavior of continuous flows, which can be stabilized by β. The necessary conditions for instability are sufficient for these profiles. Special attention was given to the existence of radiating modes when the ambient potential-vorticity gradient was non-zero (and equal to β). A definition of radiation in terms of the structure of the neutral mode contiguous to the instabilities was made.

It was found empirically that radiating instabilities exist *whenever* the range of Rossby-wave phase speeds overlaps the flow-speed range, i.e. whenever the phase-speed condition can be satisfied. In a sense, the Rossby waves of the far-field are destabilized by the localized horizontal shear. In other words, when $\beta = 0$ there is only one possible mode in the far-field and it is meridionally evanescent. This mode is unstable as long as $\beta < \beta_c$. It is just one of the many possible modes which can exist when $\beta \neq 0$: all of the others are wavelike in the meridional direction.

There is a symmetry between the results for the eastward and westward jets. In an eastward jet, Rossby waves *inside* the jet are subject to destabilization while in a westward jet, Rossby waves *external* to the jet can be destabilized. It is found that both classes of Rossby waves are destabilized by horizontal shear. However, the finite width of the jet appears to quantize the Rossby waves in the center of the eastward jet. Each cross-jet "mode" is really a discrete

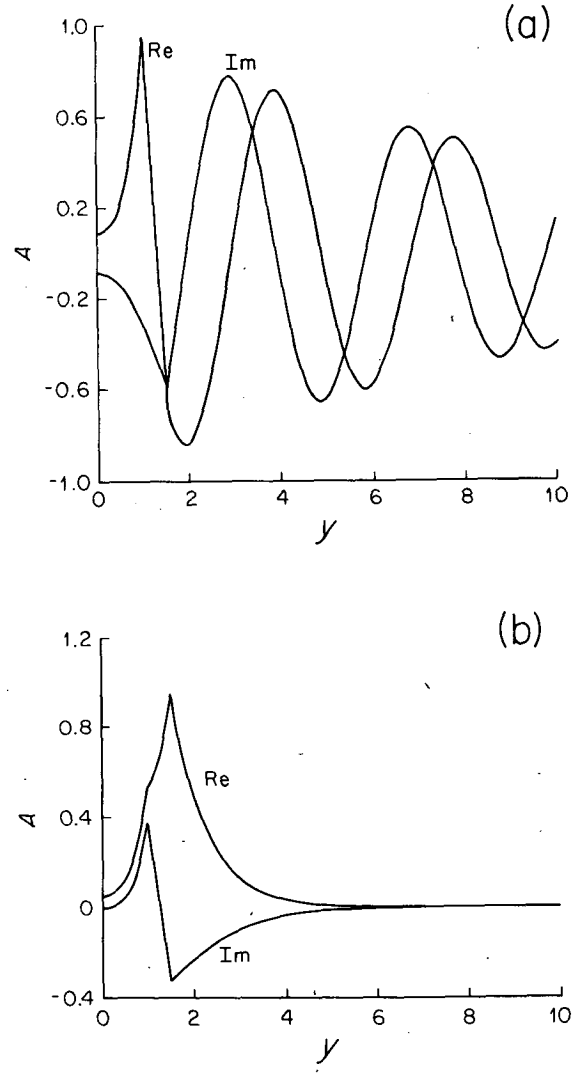

FIG. 15. Barotropic jet, sinuous mode, at $D = 1.5$ and $\beta = -2.0$: eigenfunctions for (a) $k = 0.1$ and (b) $k = 2.0$.

band of waves in β and k because of the indefinite width of the "channel". Neighboring cross-jet modes do not necessarily overlap in β and k, resulting in stable regions in the β-k plane where no cross-jet "modes" exist. Each cross-jet mode that exists for $\beta < \beta_c$ is unstable. In contrast, the far-field is semi-infinite in y, so there is a continuum of modes filling β-k plane. When the jet is westward, this continuum of far-field Rossby waves is unstable as long as $\beta < \beta_c$. Thus, when β is non-zero, the existence of additional modes that are not predicted by Howard's (1964) inflection point theorem is strongly related to the existence of wave-like solutions in y.

The relevance of these instabilities to the ocean is discussed in a second paper (Talley, 1983), in which vertical shear in the form of two layers is added to the problem discussed in the present paper. The main result of the present analysis that is of importance in the ocean and atmosphere is the proclivity of the instabilities of westward jets to radiate energy long distances from the jet while the instabilities of eastward jets are much more tightly confined. We might imagine that the nonlinear development of the instabilities and the basic flow depends on how much of the instability energy remains near the jet. If the energy is tightly confined to the jet, the possibilities of nonlinear interactions may be much greater, and in the presence of a second instability mechanism, such as baroclinic instability, these interactions may lead to prolongation and intensification of the jet. Thus, eastward jets may be more likely to be long-lived and intense than westward jets. Until a nonlinear analysis is attempted, however, this must remain a speculation.

Acknowledgments. I thank Joseph Pedlosky for suggesting the problem and for his guidance throughout. This work was part of a Ph.D. thesis in the MIT/WHOI Joint Program in Oceanography and was supported by the National Science Foundation, Office of Atmospheric Science.

REFERENCES

Dantzler, H. L., 1977: Potential energy maxima in the tropical and subtropical North Atlantic. *J. Phys. Oceanogr.*, **7**, 512–519.

Dickinson, R. E., and F. J. Clare, 1973: Numerical study of the unstable modes of a hyperbolic-tangent barotropic shear flow. *J. Atmos. Sci.*, **30**, 1035–1049.

Eady, E. T., 1949: Long waves and cyclone waves. *Tellus*, **1**, 33–52.

Fjørtoft, R., 1950: Application of integral theorems in deriving criteria of stability for laminar flow and for the baroclinic circular vortex. *Geofys. Publ.* **17**, No. 5, 52 pp., [also *Geophys. Norv.*]

Flierl, G. R., 1975: Gulf Stream meandering, ring formation and ring propagation. Ph.D. thesis, Harvard University, 270 pp.

Howard, L. N., 1961: Note on a paper of John Miles. *J. Fluid Mech.*, **10**, 509–512.

——, 1964: The number of unstable modes in hydrodynamic stability problems. *J. Mec.*, **3**, 433–443.

——, and P. G. Drazin, 1964: On instability of parallel flow of inviscid fluid in a rotating system with variable Coriolis parameter. *J. Math. Phys.*, **43**, 83–99.

Kuo, H. L., 1949: Dynamic instability of two-dimensional nondivergent flow in a barotropic atmosphere. *J. Meteor.*, **6**, 105–122.

Lindzen, R. S., and A. J. Rosenthal, 1976: On the instability of Helmholtz velocity profiles in stably stratified fluids when a lower boundary is present. *J. Geophys. Res.*, **81**, 1561–1571.

McIntyre, M. E., and M. A. Weissman, 1978: On radiating instabilities and resonant over-reflection. *J. Atmos. Sci.*, **35**, 1190–1196.

Pedlosky, J., 1964: The stability of currents in the atmosphere and the oceans. Part I. *J. Atmos. Sci.*, **21**, 201–219.

——, 1977: On the radiation of meso-scale energy in the mid-ocean. *Deep-Sea Res.*, **24**, 591–600.

——, 1979: *Geophysical Fluid Dynamics,* Springer-Verlag, Inc. New York, 624 pp.

Rayleigh, Lord, 1879: On the instability of jets. *Scientific Papers,* Vol. 1, 361–371 [Dover, 1964.]

—— 1880: On the stability, or instability, of certain fluid motions. *Scientific Papers,* Vol. 1, 474–487 [Dover, 1964.]

—— 1887: On the stability or instability of certain fluid motions, II. *Scientific Papers,* Vol. 3, 17–23 [Dover, 1964.]

Talley, L. D., 1983: Instabilities and radiation of thin, baroclinic jets. Submitted to *J. Phys. Oceanogr.*

Tung, K. K., 1981: Barotropic instability of zonal flows. *J. Atmos. Sci.*, **38**, 308–321.